引用格式：LU Xiao-tian, LI Feng, XIAO Bian, *et al*. An Effectiveness Evaluation Method for Space-based Optical Imaging Systems[J]. *Acta Photonica Sinica*, 2020, **49**(12):1212002
鲁啸天,李峰,肖变,等.天基光学成像系统探测效能评价方法[J].光子学报,2020,**49**(12):1212002

天基光学成像系统探测效能评价方法

鲁啸天[1],李峰[1],肖变[1,2],杨雪[1],辛蕾[1],鹿明[1],刘志佳[3]
(1 钱学森空间技术实验室,北京 100094)
(2 河南大学,河南 开封 475000)
(3 航天东方红卫星有限公司,北京 100094)

摘 要:提出了一种基于约翰逊准则和最小可分辨对比度的天基光学成像探测效能评价方法,综合考虑了目标和背景对比度、大气传输、探测器和人眼等诸多因素,引入噪声等效对比度来衡量探测器噪声水平,以对比度受限和分辨率受限联合概率衡量探测效能,定量直观地评价天基光学成像系统的探测能力.采用航空影像和GF-2卫星影像开展验证实验,航空影像中汽车的识别概率为46%,飞机的确认概率为73%,NIIRS等级为4.23;GF-2卫星影像中卡车的识别概率为67%,小型船的发现概率为63%,NIIRS等级为4.53.本文方法计算的探测概率和人眼主观判断基本一致,与NIIRS基本符合,证明了方法的有效性,为遥感光学探测系统设计和效能评价奠定基础.

关键词:最小可分辨对比度;噪声等效对比度;约翰逊准则;天基探测;光学成像;效能评价;GF-2
中图分类号:TP753 **文献标识码**:A **doi**:10.3788/gzxb20204912.1212002

An Effectiveness Evaluation Method for Space-based Optical Imaging Systems

LU Xiao-tian[1], LI Feng[1], XIAO Bian[1,2], YANG Xue[1], XIN Lei[1], LU Ming[1], LIU Zhi-jia[3]
(1 *Qian Xuesen Laboratory of Space Technology*, *Beijing* 100094, *China*)
(2 *Henan University*, *Kaifeng*, *Henan* 475000, *China*)
(3 *DFH Satellite Co.*, *Ltd*, *Beijing* 100094, *China*)

Abstract: A novel effectiveness evaluation method was proposed based on the Johnson criteria and minimum resolvable contrast to evaluate effectiveness. In this process, target and background contrast, atmospheric transmission, detectors, and human eyes, are considered comprehensively. The noise equivalent contrast is introduced to measure the noise level of the detector, and the detection efficiency is measured by the joint probability of contrast and resolution, which can quantitatively and intuitively evaluate the detection ability of space-based optical imaging system. Verification experiments are carried out based on aerial and GF-2 satellite images. In aerial images, the recognition probability of car is 46%, the identification probability of aircraft is 73%, and the NIIRS level is 4.23; in GF-2 satellite images, the recognition probability of truck is 67%, the detection probability of small ship is 63%, and the NIIRS level is 4.53. The results show that the probability calculated by our method is basically consistent with the

Foundation item: National Key Research and Development Projects (No. 2016YFB0501301), National Natural Science Foundation of China (No.61773383)
First author: LU Xiao-tian (1988—), male, engineer, Ph.D. degree, mainly focuses on effectiveness evaluation of detection and polarization imaging. Email: luxiaotian@qxslab.cn
Contact author: LI Feng (1975—), male, professor, Ph.D. degree, mainly focuses on remote sensing, optical image processing and reconstruction, compressed sensing and effectiveness evaluation of detection. Email: lifeng@qxslab.cn
Received: Jul.14,2020; **Accepted**: Sep.23,2020

subjective judgment of human eyes, which is basically consistent with the NIIRS. The results prove the effectiveness of the method. Our method is of great significance to the design of space-based imaging systems and the evaluation of the on-orbit satellite detection capability.

Key words: Minimum resolvable contrast; Noise equivalent contrast; Johnson criteria; Space-based detection; Optical imaging; Effectiveness evaluation; GF-2

OCIS Codes: 120.1880; 040.1880; 110.2970; 110.3000; 280.4788

0 Introduction

Optical remote sensing is extensively used in military[1], ecological[2], agriculture[3], aerospace[4], disaster reduction[5], and daily life applications[6]. The overall design of the optical remote sensing system is the most important task according to application requirements (field-of-view, meteorological and environmental conditions, characteristics of target and background, effective distance, etc.). For land-based low-light-level and infrared detection systems, there are effectiveness evaluation methods based on Minimum Resolvable Contrast (MRC)[7-8] and MRTD[8-9]. However, there is still a lack of effective means for the evaluation of the effectiveness of optical remote sensing systems. Ground Resolution Distance (GSD), Modulation Transfer Function (MTF), and the Signal-to-Noise Ratio (SNR), cannot evaluate the detection effectiveness scientifically and/or intuitively that is not conducive to system design and user use. At present, image interpretation is commonly used to evaluate the effectiveness of the detection system. The United States has studied the National Imagery Interpretability Rating Scale (NIIRS)[10] since the early 1970s. Based on these studies, the image quality can be described quantitatively. According to the interpretation task, it can be divided into different levels (0~9), and can be used as a reference to evaluate the ability of detection of different targets. However, the calculation of the NIIRS level needs an image acquired by the system for evaluation. NIIRS is the post-evaluation method and cannot provide reference for the system demonstration and design. Moreover, the NIIRS level is not specific, and the quantification is not adequately precise. The Johnson criteria is a method used for the prediction of the probability of target discrimination. When the human eye searches for the target in a certain background or on the display, the continuous response of the eye can be divided into three stages: detection, recognition, and identification. The different stages correspond to different discrimination measures. Discrimination measures combine the effectiveness of system with human vision. Discrimination measures need to be quantified using visual psychological experiments. Johnson combined target detection with equivalent bar detection based on experiments[11-12]. It is possible to evaluate the detection ability of the imaging system with target equivalent bar resolution without considerations of the nature of the target and image defects. Johnson validated the fact that the equivalent bar resolution can be used to predict the probability of target discrimination, and determined the criteria pertaining to the cycles of the equivalent bar for different discrimination measures. Johnson criteria has been extensively used worldwide.

Therefore, on the basis of considering target and background contrast, atmospheric transmission, detectors and human eyes, and Noise Equivalent Contrast (NEC)[13], this study establishes a new effectiveness evaluation method of an optical imaging system based on the Johnson criteria and MRC that was designed and implemented for a space-based optical imaging system. This method can evaluate the effectiveness quantitatively and intuitively, which is close to the actual needs. Additionally, our method can calculate the probability of detection, recognition, and identification of targets in typical backgrounds based on given parameters in the demonstration stage to guide the selection of the remote sensing detector. It is of great significance to the design of a space-based imaging system and the evaluation of on orbit satellite detection capability.

1 Evaluation method for the effectiveness of a space-based optical imaging system

1.1 NEC

To facilitate the establishment of an MRC model, we introduce the concept of NEC. In the photoelectric imaging system, when the output signal of the reference electronic filter equals the root-mean-square of the noise of the system itself, the contrast between the target and the background is the noise equivalent contrast.

The SNR from the reference electronic filter can be expressed as

$$\mathrm{SNR}=\frac{S}{N}=\frac{\Delta\Phi(\lambda)R(\lambda)}{\sqrt{\int_0^{\infty}s'(f)\mathrm{MTF}_{\mathrm{e}}^2(f)\mathrm{d}f}} \tag{1}$$

where $\Delta\Phi(\lambda)$ is radiation flux difference between the target and background, $R(\lambda)$ is the responsivity of the detector, $s'(f)$ is the noise power spectrum of the detector, $\mathrm{MTF}_{\mathrm{e}}(f)$ is the MTF of the electronic filter.

$$\Delta\Phi(\lambda)=\frac{1}{4}\Delta E(\lambda)A_{\mathrm{d}}\tau_0(\lambda)\left(\frac{D}{f_0'}\right)^2\Bigg/\left[1+\frac{1}{4}\left(\frac{D}{f_0'}\right)^2\right] \tag{2}$$

where $\Delta E(\lambda)$ is the irradiance difference between the reflected light of target $E_{\mathrm{t}}(\lambda)$ and background $E_{\mathrm{b}}(\lambda)$ at the entrance pupil, is the pixel area of the detector, $\tau_0(\lambda)$ is the transmittance of the optical system, D is the aperture, and f_0' is the focal length.

According to the definition of NEC, Eq. (1) is assumed to be equal to unity,

$$\Delta E(\lambda)=\frac{4F^2\left(1+\frac{1}{4F^2}\right)\sqrt{\Delta f_{\mathrm{n}}}}{R(\lambda)A_{\mathrm{d}}\tau_0(\lambda)} \tag{3}$$

$$\Delta f_{\mathrm{n}}=\int_0^{\infty}s'(f)\mathrm{MTF}_{\mathrm{e}}^2(f)\mathrm{d}f \tag{4}$$

$$\mathrm{NEC}=\frac{\Delta E(\lambda)}{E_{\mathrm{t}}(\lambda)+E_{\mathrm{b}}(\lambda)} \tag{5}$$

where Δf_{n} is the noise equivalent bandwidth, and $F=D/f_0'$. In fact, the nature of NEC is to measure noise based on the intensity of the input signal. In the case of Charge-Coupled Device (CCD) Complementary Metal-Oxide Semiconductor (CMOS) detectors, in addition to the inherent shot noise that is related to the number of charges produced by photoelectric effect, the readout noise should also be considered.

On the basis of the NEC model, the MRC model is also deduced as described in the next subsection.

1.2 MRC

MRC is defined as the contrast between the target and the background when the observer can barely distinguish the bars at a specific spatial frequency. It is an evaluation parameter that can describe quantitatively the threshold contrast of the visible photoelectric imaging system. It includes the factors of sensitivity, noise, spatial frequency, and human eyes. It can fully reflect the detection ability of the photoelectric imaging system.

The process of MRC derivation is as follows. The SNR received by the system can be described as

$$\mathrm{SNR}_0=\frac{C}{\mathrm{NEC}} \tag{6}$$

where C is the contrast between the target and the background. The SNR of the image on the display is

$$\mathrm{SNR}_i=\mathrm{SNR}_0\cdot R(f)\left[\Delta f_{\mathrm{n}}\Big/\int_0^{\infty}s(f)\mathrm{MTF}_{\mathrm{m}}^2(f)\mathrm{d}f\right]^{1/2} \tag{7}$$

where $R(f)$ is the square wave response of the system, $\mathrm{MTF}_{\mathrm{m}}(f)$ is the modulation transfer function of the section behind the readout circuit, and $s(f)$ is the noise power spectrum. According to the relationship between $R(f)$ and $\mathrm{MTF}_{\mathrm{s}}(f)$, and based on the approximation of the first term,

$$R(f)\approx\frac{4}{\pi}\mathrm{MTF}_{\mathrm{s}}(f) \tag{8}$$

When the observer observes the target, the human eye will modify the SNR according to the following four aspects[14-15]

1) The eye extracts the strip pattern. When the signal is distinguishable, the high-order harmonic is filtered out and the first-order harmonic is maintained. The peak value of the signal is then attenuated as follows

$$\frac{2}{\pi}R(f)=\frac{8}{\pi^2}\mathrm{MTF}_{\mathrm{s}}(f) \tag{9}$$

2) Because of the time integration, the signal will be sampled independently according to the integral time of the human eye ($t_e = 0.2$ s), while noise will be superimposed at the same time. Therefore, the SNR will be improved $(t_e f_p)^{1/2}$, whereby f_p is the frame rate of display.

3) In the vertical direction, the eye will integrate the signal in the spatial domain, and will use the instantaneous vertical field-of-view β as the correlation length of the noise. Thus, the SNR will be improved according to

$$\left(\frac{L}{\beta}\right)^{1/2} = \left(\frac{\varepsilon_0 W}{\beta}\right)^{1/2} = \left(\frac{\varepsilon_0}{2 f_T \beta}\right)^{1/2} \tag{10}$$

where L and W are the angle length and angle width of the strips, respectively, and $\varepsilon_0 = L/W$, $f_T = 1/(2W)$.

4) For the periodic rectangular strip target with frequency f_T, the narrow-band spatial filtering effect of the human eye is equivalent to the matched filter whose transfer properties can be expressed as $\mathrm{sinc}^2(\pi/2 \cdot f/f_T) \cdot \mathrm{MTF}_s^2(f)$, where f represents the spatial frequency. Therefore, the integral response of the human eye can be converted into the noise bandwidth Δf_{eye} considering the human eye matching filter according to the actual system bandwidth

$$\Delta f_{eye} = \int_0^\infty s(f)\,\mathrm{MTF}_s^2(f)\,\mathrm{MTF}_{eye}^2(f)\,\mathrm{sinc}^2\left(\frac{\pi}{2}\frac{f}{f_T}\right)\mathrm{d}f \tag{11}$$

where $\mathrm{MTF}_{eye}(f)$ is the modulation transfer function of the human eye, and $\mathrm{sinc}(\cdot)$ is the sine basis function. As f_T goes to zero, Δf_{eye} approaches the target frequency f_T (assuming white noise)[9].

Combining the four aforementioned corrections with the SNR_t, the visual SNR can be obtained as

$$\mathrm{SNR}_v = \frac{8}{\pi^2}\mathrm{MTF}_s(f)\mathrm{MTF}_{eye}(f)\,\frac{C\left(t_e f_p\right)^{1/2}}{\mathrm{NEC}}\left(\frac{\varepsilon_0}{2 f_T \beta}\right)^{1/2}\left(\frac{\Delta f_n}{\Delta f_{eye}}\right)^{1/2} \tag{12}$$

Let SNR_v be equal to the threshold SNR such that the human eye can distinguish the strip SNR_{DT}. At this time, C is the MRC.

$$\mathrm{MRC} = \frac{\pi^2}{8}\frac{\mathrm{SNR}_{DT} \times \mathrm{NEC} \cdot f_T}{\mathrm{MTF}_s(f)\mathrm{MTF}_{eye}(f)}\left(\frac{2\beta}{\varepsilon_0 t_e f_p}\right)^{1/2}\left(\frac{1}{\Delta f_n}\right)^{1/2} \tag{13}$$

Based on practical applications, the MRC model needs to be modified:

1) Correction of ε_0

The ratio of length to width of the common strips in laboratory is 7∶1 (or 5∶1). However, ε_0 is not only related to the target itself, but it is also related to the number of cycles for 50% detection according to the Johnson criteria. Therefore, the ratio of the length-to-width after the correction ε is,

$$\varepsilon = (2nL/W)/7 \tag{14}$$

where n is the number of cycles for 50% detection, as shown in Table 1.

Table 1 Johnson criteria

Discrimination measure	Description	One-dimensional (1-D) criteria (number cycles) n	Two-dimensional (2-D) criteria (number cycles) n
Detection	Blob has a reasonable probability of being the sought object	1.0	0.75
Recognition	Object discerned with sufficient clarity such that its specific class can be differentiated (tank, truck, man)	4.0	3.0
Identification	Object discerned with sufficient clarity to specify the type within a class (T-62, T-72, M1 tanks)	8.0	6.0

2) Δf_n correction

In practice, only the dark current noise of the detector is considered, while the dark current noise has a fixed value, that is, NEC is only related to the irradiance of the target and background, but it is also affected by

the integration time in practice. Therefore, it needs to be corrected. Herein, we used the multiple t_n of integral time to improve SNR instead of Δf_n.

The final MRC can be derived as

$$\mathrm{MRC}=\frac{\pi^2}{8}\frac{\mathrm{SNR_{DT}}\times\mathrm{NEC}\cdot f_T}{\mathrm{MTF_s}(f)\mathrm{MTF_{eye}}(f)}\left(\frac{2\beta}{\varepsilon t_e f_p}\right)^{1/2}\left(\frac{1}{t_n}\right)^{1/2} \tag{15}$$

1.3 Detection efficiency evaluation method based on the combination of MRC and Johnson criteria

By substituting MRC and the contrast between the target and background C_0 into the target transfer probability function[12], the contrast limited probability P_C can be obtained as

$$P_C=\frac{\left(C_0/\mathrm{MRC}\right)^{E_C}}{1+\left(C_0/\mathrm{MRC}\right)^{E_C}} \tag{16}$$

where $E_C=2.7+0.7(C_0/\mathrm{MRC})$.

By substituting the resolvable cycles N across the target and n into the target transfer probability function, the resolution limited probability P_J is obtained.

$$P_J=\frac{\left(N/n\right)^{E_J}}{1+\left(N/n\right)^{E_J}} \tag{17}$$

where $E_J=2.7+0.7(N/n)$.

Finally, the probability of detection is

$$P=P_C\cdot P_J \tag{18}$$

The flow diagram of the proposed method is shown in Fig.1.

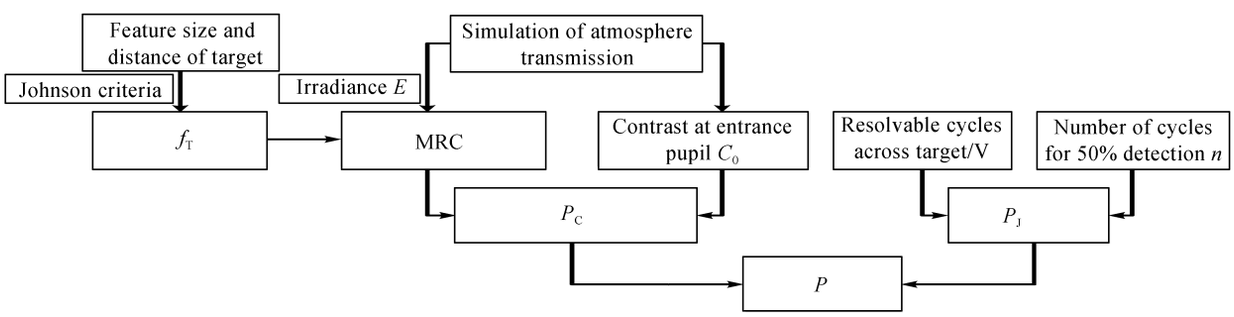

Fig. 1 Flow diagram of our proposed method

2 Experimental verification and analysis

2.1 Experimental verification with aerial images

An aviation detection experiment was carried out in Jingmen, Hubei Province on May 20, 2019. The weather was clear on that day, the visibility was 23 km, the time was 9:30 a.m., and the solar altitude angle was 40°. The relevant parameters of the detector for the aviation detection experiment are shown in Table 2. The radiance values of the target (small vehicle) and background (cement pavement) obtained with the atmospheric transmission simulation software were $L_t=0.003\ 72\ \mathrm{W/cm^2/sr}$ and $L_b=0.001\ 56\ \mathrm{W/cm^2/sr}$, respectively. The NEC was 0.003 2. The width and length of the target (a car is shown in Fig.2) were 4.8 m and 1.7 m, respectively. We used 2-D criteria in Table 1, n=[0.75 3 6], where the three numbers represented the levels of detection, recognition, and identification, respectively. We obtained the MRC=[0.0097 0.019 0.027] according to Eq. 15. According to Eqs. (16)~(17), we obtained P_C=[1.00 1.00 1.00] and P_J=[1.00 0.46 0.10]. Finally, P=[1.00 0.46 0.10], therefore, the probabilities of detection, recognition, and identification, were 100%, 46%, and 10%, respectively. It was worth noting that the contrast-limited probability P_C was [1.00 1.00 1.00]. This means that the contrast was adequate to visualize the target at this time. Accordingly, the contrast was not the main factor that affected the probability. Obviously, cars can be easily detected in the aerial image shown in Fig. 2 (the probability of detection was 100%). Furthermore, we

can recognize it as a car (the probability of recognition was 46%) but we cannot identify the specific type of the car (the probability of identification was10%). At this point, the NIIRS was 4.23. Similarly, the probability of the aircraft in Fig.2(b) was [1.00 0.92 0.73], i.e., the aircraft can be detected, recognized, and identified. The P_C and P_J were [1.00 0.92 0.73] and [1.00 1.00 0.98], the results showed that the resolution was good enough to visualize the target at this time. It can be observed in Fig.2(b) that the gray level values of the aircraft and the ground were almost the same, and the contrast was low. Thus, the contrast was the main factor responsible for probability changes. Our calculation results were consistent with the subjective observation and NIIRS. The results showed that our method was effective and accurate.

Table 2 The relevant parameters of aviation experiment

Parameter name	Number	Parameter name	Number
Diameter of aperture	20 mm	Focal length	5 mm
Transmittance of optical system	0.7	GSD	0.5 m
Height	586 m	SNR_{DT}	2.25

(a) Car (b) Aircraft

Fig. 2 Aerial image of ground target

2.2 Experimental verification with GF-2 satellite images

The GF-2 satellite is the first civil optical remote sensing satellite developed by China with a spatial resolution better than 1 m. The resolution of the sub-satellite point can reach a value of 0.8 m. The main technical parameters are shown in Table 3. We used the targets on the land and marine images of GF-2 to carry out the verification experiments.

Table 3 Main technical parameters of GF-2 satellite

Parameter name	Number	Parameter name	Number
Relative aperture	1/15	MTF	0.12
Focal length	7.8 m	GSD	0.8 m
Orbital height	631 km	SNRDT	2.25
Dynamic range	≥25 dB (θ=20°,ρ=0.05);≥46 dB (θ=70°,ρ=0.65)		

Notes: θ is solar elevation; ρ is surface albedo.

We selected a car and a truck as the targets in Fig.3. The size of the car is 4.8 m×1.7 m (length × width, the same below), and the probability P was [1.00 0.32 0.05]. In addition, the size of the truck is 17.5 m×1.8 m with probabilities P of [1.00 0.67 0.17]. It is worth noting that the observer had prior knowledge, therefore, sometimes even a small recognition probability can have profound effects. For example, when the recognition

probability of a car is 0.32, the car can be hardly recognized. However, when it is on the road, it is easier to be recognized as a car. The NIIRS level of Fig.3 is 4.53, which is basically consistent with our method.

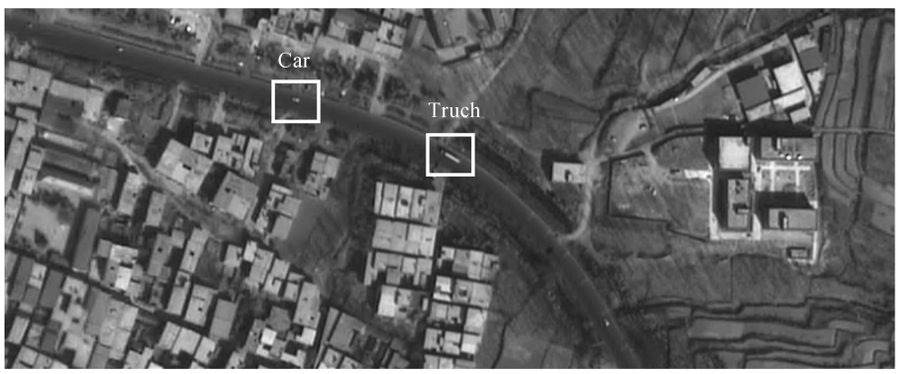

Fig. 3 GF-2 image of city

In the marine image, we chose large and small civilian ships as targets, as shown in Fig.4. The probability of the large ship 88.8 m×15.8 m was [1.00 1.00 1.00], while the probabilities of the small ships 1 34.4 m×8.0 m and 2 16.8 m×4.8 m were [0.98 0.63 0.31] and [0.62 0.14 0.03], respectively. The NIIRS level of Fig.4 is 4.53, which is basically consistent with our method.

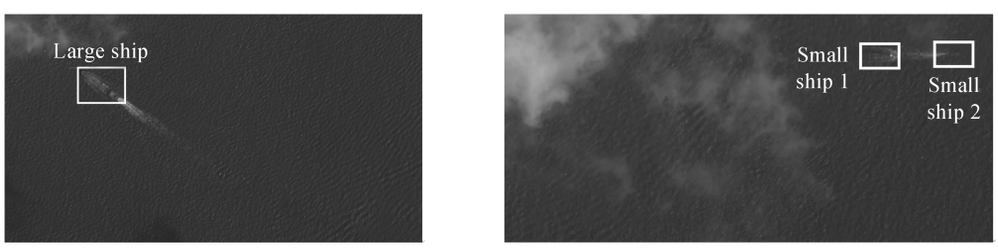

(a) Large ship, 88.8 m×15.8 m (b) Small ships, 34.4m×8.0m and 16.8 m×4.8 m

Fig. 4 GF-2 marine images

In general, the detection probability calculated by our method is in good agreement with the subjective judgment of human eye observations.

3 Conclusions

In this study, a new effectiveness evaluation method was proposed for space-based optical imaging systems to evaluate the effectiveness of optical detection based on the Johnson criteria and MRC. Compared with traditional methods, our method took the characteristics of target and background, atmospheric transmission, detectors, and human eyes into considerations. Additionally, our method can calculate the probability of detection, recognition, and identification of targets in typical backgrounds based on given parameters in the design stage to guide the selection of the remote sensing detectors. Experimental results showed that the detection probability calculated by our method is in good agreement with the subjective judgment of human eye observation. We have prepared 100 subjective experiment sample bank of different scale targets, and will carry out a large number of subjective experiments in the future to verify the correctness of our method.

However, this method does not consider subjective factors, such as the experience and ability of observers, and thus needs to be improved by combining it with deep learning and artificial intelligence technologies. It is also necessary to study the noise types of different detectors and optimize the detection efficiency evaluation model. These constitute work-in-progress and are envisaged to constitute the topics of our future research publication.

References

[1] ALLISON R S, JOHNSTON J M, CRAIG G, *et al*. Airborne optical and thermal remote sensing for wildfire detection and monitoring[J]. *Sensors*, 2016, **16**(8): 1310.

[2] VERRELST J, CAMPS-VALLS G, MUÑOZ-MARÍ J, *et al*. Optical remote sensing and the retrieval of terrestrial vegetation bio-geophysical properties - A review[J]. *ISPRS Journal of Photogrammetry and Remote Sensing*, 2015, **108**: 273-290.

[3] KHANAL S, FULTON J, SHEARER S. An overview of current and potential applications of thermal remote sensing in precision agriculture[J]. *Computers and Electronics in Agriculture*, 2017, **139**: 22-32.

[4] CHENG G, HAN J. A survey on object detection in optical remote sensing images[J]. *ISPRS Journal of Photogrammetry and Remote Sensing*, 2016, **117**: 11-28.

[5] VASSILEVA M, GIULIO TONOLO F, RICCARDI P, *et al*. Satellite SAR interferometric techniques in support to emergency mapping[J]. *European journal of remote sensing*, 2017, **50**(1): 464-477.

[6] JOSHI N, BAUMANN M, EHAMMER A, *et al*. A review of the application of optical and radar remote sensing data fusion to land use mapping and monitoring[J]. *Remote Sensing*, 2016, **8**(1): 70.

[7] LIU Song, JIN Wei-qi, LI Li, *et al*. Minimum resolvable contrast measurement of low illumination imaging module and simulation of its range[J]. *Acta Photonica Sinica*, 2016, **45**(3): 0312003.

[8] LUO Hua, ZHANG Yuan. Evaluation of imaging quality of CCD cameras by measuring minimum resolvable contrast[J]. *Acta Photonica Sinica*, 2009, **38**(3): 681-684.

[9] RATCHES J A. Static performance model for thermal imaging systems[J]. *Optical Engineering*, 1976, **15**(6): 156525.

[10] ABOLGHASEMI M, ABBASI-MOGHADAM D. Conceptual design of remote sensing satellites based on statistical analysis and NIIRS criterion[J]. *Optical and Quantum Electronics*, 2015, **47**(8): 2899-2920.

[11] SJAARDEMA T A, SMITH C S, BIRCH G C. History and evolution of the Johnson criteria[C]. SANDIA Report, 2015: SAND2015-6368.

[12] DRIGGERS R G, COX P G, KELLEY M. National imagery interpretation rating system and the probabilities of detection, recognition, and identification[J]. *Optical Engineering*, 1997, **36**(7): 1952-1959.

[13] DEWEERT M J, COLE J B, SPARKS A W, *et al*. Photon transfer methods and results for electron multiplication CCDs [C]. Applications of Digital Image Processing XXVII, International Society for Optics and Photonics, 2004, **5558**: 248-259.

[14] LLOYD J M. Thermal imaging systems[M]. Springer Science & Business Media, 2013.

[15] DUDZIK M C. Electro-optical systems design, analysis, and testing[C]. SPIE, 1993, **4**: 245-298.